NUMERICAL ASSESSMENT OF FLUID FLOW AND OXYGEN AVAILABILITY IN THE AMC BIOARTIFICIAL LIVER

Guy Mareels*, Paul Poyck**, Sunny Eloot*, Robert A.F.M. Chamuleau**, Pascal R. Verdonck*

* Cardiovascular Mechanics and Biofluid Dynamics Research Group, Institute of Biomedical Technology, Ghent University, Gent, Belgium
** Departments of Experimental Surgery and Hepatology, Academic Medical Center, University of Amsterdam, Amsterdam, The Netherlands

Guy@navier.ugent.be

Abstract: A future therapy for liver failure may be the use of a bioartificial liver (BAL). This device employs living liver cells to support the failing liver. The cells should be adequately perfused to provide them with sufficient oxygen and other metabolites. In this study, a fully parametric model of the AMC-BAL (Amsterdam Medical Center, Amsterdam, The Netherlands) was developed to allow computational fluid dynamics (CFD) simulations of fluid flow and oxygen transport and consumption inside the AMC-BAL. Simulation results show a good distribution of the flow across the AMC-BAL, despite the presence of a preferential flow path. Oxygen levels are highest near the gas capillaries and decrease with increasing distance from the capillaries. The preferential flow path however causes a decrease in convective oxygen supply to the hepatocytes. Adoption of this information can be used to further optimize the efficiency of the BAL. The developed models are useful to analyze and further optimize O_2 transport in the AMC bioartificial liver and in other bioreactors.

Introduction

Acute liver failure (ALF) is a severe disease with high mortality rates (60-90%) [1,2]. At present, the only efficient therapy is orthotopic liver transplantation (OLT) [3]. Shortage of suitable donor livers, however, has created the need for an artificial liver that can bridge the patient to transplantation or to regeneration of the diseased liver. The most promising solution for the treatment of ALF patients are bioartificial liver (BAL) systems. These systems are extracorporeal devices that are generally comprised of a bioreactor in which living hepatocytes (liver cells) are seeded. In a clinical setting, toxic plasma of ALF patients is perfused through the bioreactor and detoxified by the viable hepatocytes. A major advantage of BAL systems, as compared to other artificial liver support systems, is the capacity to provide a full range of metabolic functions to compensate for the complex metabolic disorders seen in ALF. In vitro BAL studies have shown that liver specific functions are well maintained for several weeks. But despite this potential of long-term in vitro functionality, none of the present BAL systems have proven to effectively bridge ALF patients to transplantation or regeneration in a randomized controlled clinical trial. Reasons for this discrepancy can be an impairment in the local flow of plasma or oxygen transport inside the bioreactor. To maintain optimal cell function and detoxifying capacity, it is of utmost importance that the bioreactor is adequately perfused with plasma in order to supply sufficient nutrients (glucose), oxygen and unwanted metabolites (e.g. ammonia) to the cells and to remove all metabolic end products (e.g. CO2, urea). However, high flow rates lead to elevated cellular shear stresses, which are unfavorable for the function and viability of hepatocytes. Oxygen (O2) transfer is considered as the main limitation in the efficiency of a bioartificial liver [4], particularly due to its low solubility in plasma and the high demand for oxygen of functionally active hepatocytes. Therefore, the development of a complete detailed full-scale computer model of the BAL geometry and subsequent computational fluid dynamics (CFD – Fluent 6, Fluent Inc., Sheffield, UK) simulations could provide insight in the local flow field and oxygen availability. This information can be used to determine the optimal working parameters and to further optimize the design of a bioartificial liver.

As a research subject in this study, the AMC-bioartificial liver (AMC-BAL; Academic Medical Center, Amsterdam, The Netherlands) was considered for its innovative design and promising results as has been shown in in vitro set-ups, small and large animal ALF models, and finally in a phase I clinical study with ALF patients [5-7].

Materials and Methods

The AMC-BAL comprises a cylindrical polycarbonate housing (fig.1-A) in which two pieces of three-dimensional (3D) non-woven polyester matrix mat (fig.1-e/g; fig.1-B) are spirally wound around a massive inner core (fig.1-E). A space between the two mat segments (fig.1-f) is left open for an additional hepatocyte seeding port (not shown). In the hydrophilic matrix, high-density hepatocyte culture is possible. Between the windings of the matrix, hydrophobic gas capillaries (fig.1-C; fig.2) are positioned along the entire

ISSN: 1727-1983

bioreactor to supply additional oxygen to the hepatocytes. Plasma enters the inflow zone (fig.1-j) of the AMC-BAL through an inflow port (fig.1-b), flows through the void space between the matrix windings and the gas capillaries (fig.1-D; fig.2) in the two mat segments and flows out of the bioreactor past the outflow zone (fig.1-k) through the outflow port (fig.1-d). Unlike in hollow fiber type BALs, the hepatocytes are in direct contact with the patient's plasma in order to enhance bidirectional solute exchange between the hepatocytes and the perfused medium.

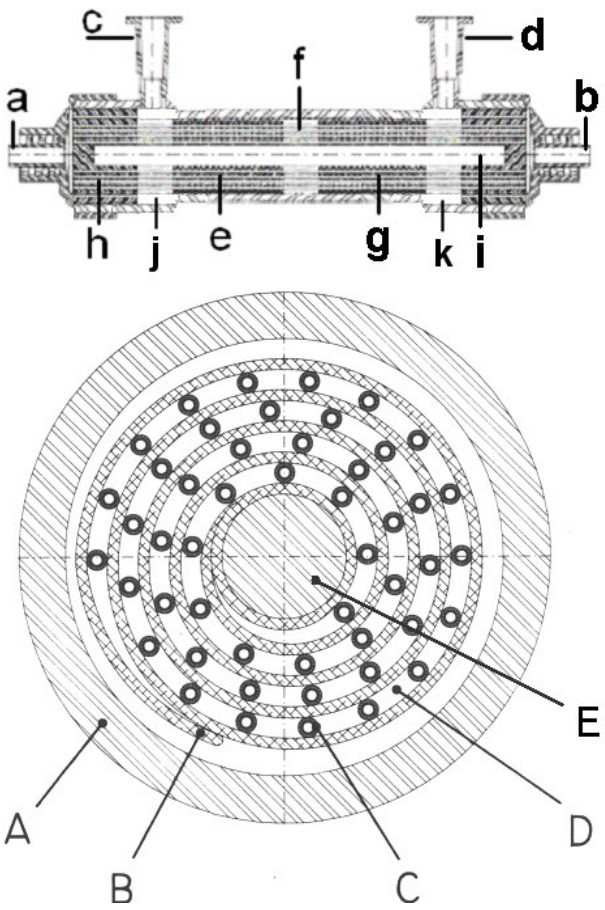

Figure 1 : Design of the laboratory scale AMC-BAL. UP: longitudinal view (a = gas outlet; b = gas inlet; c = plasma inlet; d = plasma outlet; e = first mat segment; f = interspace; g = second mat segment; h = polyurethane potting to separate gas and fluid compartment; i = inner core; j = inflow zone; k = outflow zone); DOWN: transverse view through mat segment (A = polycarbonate housing; B = non-woven polyester matrix mat; C = gas capillaries; D = inter-capillary space through which plasma flows; E = massive polycarbonate inner core).

A typical research scale AMC BAL has 2 sets of 11 spiral matrix windings (thickness = 400µm, length = 50 mm) with a 6 mm interspace between them. About 300 oxygen capillaries (outer diameter = 380µm) run in-between the windings in a more or less equidistant arrangement.

Figure 2: Close up of the non-woven polyester matrix and the oxygen capillaries with void spaces for plasma flow in between.

For the analysis of fluid flow and oxygen transport, a computer model of the AMC-BAL has to be developed. Due to the extent and the complexity of the geometry, the model creation in Gambit 2 (Fluent Inc., Sheffield, UK) has been automated using Matlab (The Mathworks, Natick, MA, USA) generated journal files. This allows the time-efficient construction of a fully parametric model in which virtually every dimension and design parameter (number of spiral layers and capillaries, capillaries' position) can be altered. As such, future parametric design studies are possible.

The AMC BAL computer model was created without explicitly drawing the spiral matrix sheet in order to facilitate and speed up the model construction. Instead, using a user-defined function in the computational software, the grid-cells that describe the spiral matrix were marked. The non-woven polyester mat was modelled as a homogeneous porous medium. In Fluent, porous media are modelled by the addition of a momentum source term to the standard fluid flow equations. This source term is thus only activated in the marked grid cells.

The source term (Eq. 1) comprises a viscous loss term (first term - proportional to the velocity) and an inertial loss term (second term - proportional to the velocity squared).

$$S_i = -\left(\frac{\mu}{\alpha} v_i + C\frac{1}{2}\rho|v|v_i\right) \qquad (1)$$

In Eq. 1, $1/\alpha$ is the viscous inertial resistance factor and C is the inertial resistance factor. An experimental setup was constructed (Fig. 3) to determine these parameters by establishing the pressure drop – flow rate relationship of the non-woven polyester matrix fabric.

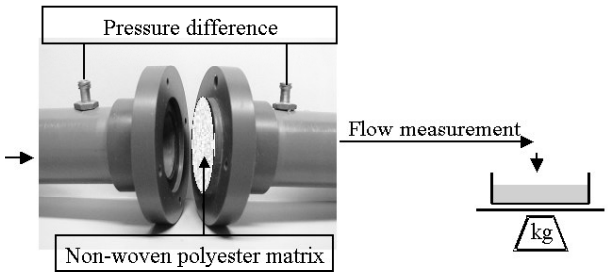

Figure 3 : Experimental setup used to determine the hydraulic permeability of the non-woven polyester matrix

ISSN: 1727-1983

A piece of the matrix fabric sheet was clamped between two connecting tubes through which flowed de-ionized water. The flow rate was imposed by adjusting the height of a constant level water reservoir (not drawn) and was measured gravimetrically. The corresponding pressure difference over the matrix sheet was measured using a calibrated differential pressure transducer. The measurements were performed twice with a complete rebuild of the setup in between to check reproducibility. Then by using regression, the best fitting relation between the measured pressure difference (30 – 80 Pa) and the applied average flow velocity (1 – 7 mm/s), was determined (Eq. 2).

$$\Delta p = c_1 v + c_2 v^2 \qquad (2)$$

From the results it could be concluded that c_2 could be neglected, indicating that the measurements were still in the linear range. This is plausible since the range of velocities through the mat in the experiment were very low (Reynolds number << 10). As a result, the inertial loss term in Eq. 1 was discarded. Subsequent linear regression resulted in the parameter c_1. From $c_1 = \frac{\mu}{\alpha} \cdot n$ (n = mat thickness), the viscous resistance factor was calculated to be $2.7 * 10^{10}$ m^{-2}.

To simulate fluid flow, Fluent 6 (Fluent Inc., Sheffield, UK) numerically solves the Navier-Stokes equations. Plasma was modelled as an incompressible, Newtonian fluid (density ρ = 1030 kg/m^3, dynamic viscosity μ = 1.2 mPa.s). Simulations were under isothermal conditions. Inlet boundary conditions were set as velocity inlets, outlet boundary conditions were set to a zero pressure outflow. The capillary and outer housing walls were no-slip walls. Total mass flow rate for the model was 10 ml/min.

To model oxygen transport, Fluent solves the convection-diffusion equation (Eq. 3).

$$\frac{\partial}{\partial x_i}(\rho u_i \phi - \rho D \frac{\partial \phi}{\partial x_i}) = S_\phi \qquad (3)$$

The transported scalar ϕ is the product of the oxygen solubility α and the local oxygen partial pressure (pO2). Oxygen solubility α in plasma is $2.855\ 10^{-5}$ ml O_2 / mmHg*ml fluid. Oxygen diffusion coefficient D is set to $2.2\ 10^{-9}$ m^2/s in the free fluid zone. Since hepatocytes tend to reduce oxygen permeability, the oxygen diffusion constant was reduced to $1.6\ 10^{-9}$ m^2/s in the hepatocyte-filled mat zone. The plasma inflow carries 150 mmHg O_2 partial pressure. Through the gas capillaries runs a 95-5% air-CO2 mixture. This is modelled by imposing a constant 150 mmHg O_2 partial pressure on the outer surface of the capillaries.

The oxygen consumption of the hepatocytes The O2 consumption by the hepatocytes is modelled by implementing an additional source term S_ϕ which is only activated in the mat zone (which contains the hepatocytes). The source term (Eq. 4) is based on non-linear Michaelis-Menten kinetics of O_2 consumption by hepatocytes, which expresses the reaction rate of an enzymatic reaction (i.e. O2 consumption) as a function of the substrate (i.e. O2) concentration.

$$-V_M \frac{p_{O2}}{p_{O2} + K_M} \qquad (3)$$

Michaelis-Menten parameters for porcine hepatocyte O_2 consumption are obtained from [8]. The maximum O_2 consumption rate V_M = 0.3 nmole / (s*10^6 cells) and the Michaelis-Menten constant K_M = 0.5 mmHg. The matrix mat is seeded with one billion porcine hepatocytes resulting in a hepatocyte cell density of 44 10^6 cells/cm^3.

Results and discussion

A fully parametric 3D model of the AMC BAL was developed to allow future parametric design studies. Figure 4 shows a colorimetric contour plot of flow velocities in a transverse plane through a mat segment.

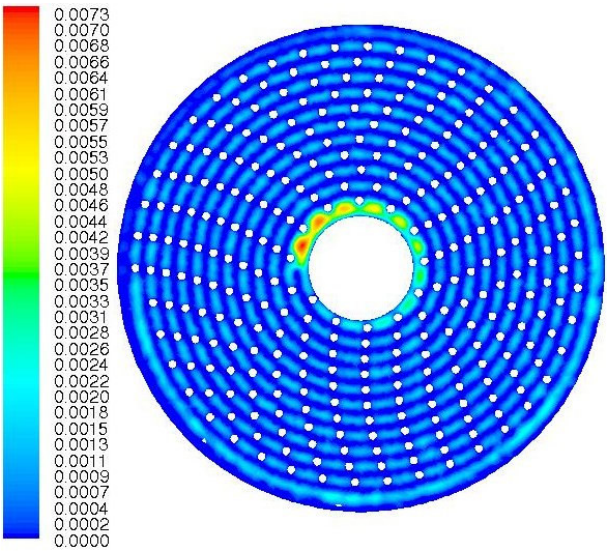

Figure 4: Contour plot of velocity magnitudes in a transverse plane through a mat segment (m/s).

The shape of the spiral matrix is very well noticeable: the velocities through the matrix sheet are an order of magnitude smaller than the velocities through the open zones between the spiral windings and the gas capillaries. The distribution of flow rate across the many free flow zones is very homogeneous. Only near the inner core, the presence of a preferential flow path (fig.4) can be noticed. Velocities there are 4-6 times higher than in the other free flow zones. This is due to the fact that the spiral matrix is not fully attached to the core and leaves a gap in between. This type of gap has already been noticed in the AMC-BAL. This kind of preferential flow will diminish the amount of flow that runs through the other free flow zones to perfuse the hepatocytes.

ISSN: 1727-1983

Figure 5 shows the distribution of oxygen partial pressure (pO_2) in a longitudinal plane through the bioreactor.

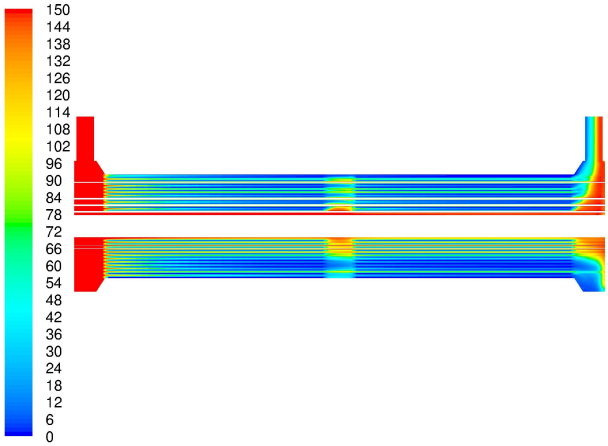

Figure 5 : Contour plot of oxygen partial pressure in a longitudinal plane of the AMC-BAL (mmHg).

At the left (fig.5) the plasma enters the bioreactor at 150 mmHg and enters the first mat segment where there is a certain decline in pO_2 noticeable due to the presence of the hepatocytes. In the zone between the two mat segments the average pO_2 increases due to the gas capillaries and the absence of hepatocytes, but then further decreases in the second hepatocyte-filled mat segment. In the outflow zone the average pO_2 is again increased by the gas capillaries up to 60 mmHg at the outlet.

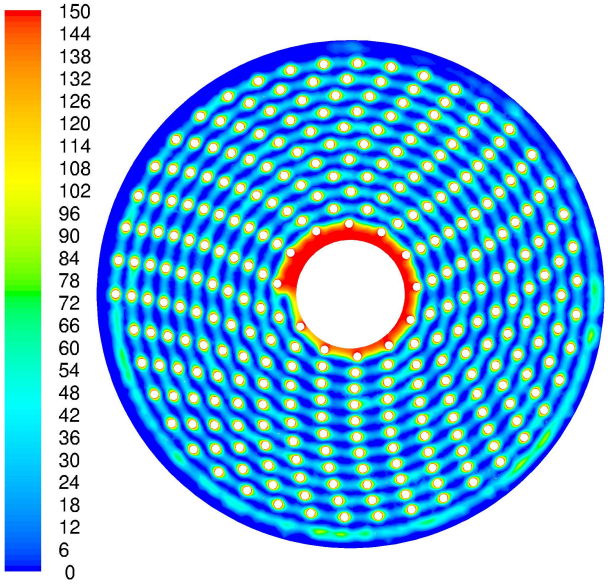

Figure 6 : Contour plot of pO_2 in a transverse plane through the first mat segment (mmHg).

Figure 6 shows the pO_2 in a transverse plane through the first mat segment. The highest pO_2 values are located around a capillary and decrease with increasing distance to the capillary. This situation is repeated across the entire cross-section.

It is clear that certain zones in the spiral mat are totally deprived of oxygen. Limited oxygen content is however still present in the fluid zones between the spiral windings and the capillaries. The preferential flow path that was shown in figure 4 is also visible in the pO_2 distribution. The oxygen content of this flow is not used to oxygenate the hepatocytes and remains almost at its initial pO_2 level.

As was shown in figure 5, an analogous cross-section of the second mat segment will show an analogous pO_2 distribution but with lower average pO_2 values.

Conclusions

A fully parametric 3D computer model of the AMC BAL bioreactor was developed, allowing future parametric design studies. The fluid flow distribution is homogeneous across the AMC-BAL with the exception of a preferential flow path near the inner core. The oxygen distribution is considered to be repetitive with highest pO_2 levels near the capillaries and declining further away from the capillaries. The preferential flow path renders a considerable part of the convective oxygen supply that is carried with the incoming plasma useless to the hepatocytes. Adjusting the manufacturing process to compensate for the gap between the spiral mat and the inner core may prevent such preferential flow and add to the oxygen supply of the hepatocytes, further increasing their possible survival.

It can be concluded that the developed models are useful to analyze and further optimize O_2 transport in the AMC bioartificial liver and in other bioreactors.

References

[1] S. De Rave, H. W. Tilanus, J. Van der Linden, R. A. De Man, B. Van der Berg, W. C. Hop, J. N. Ijzermans, P. E. Zondervan and H. J. Metselaar, (2002): *The importance of orthotopic liver transplantation in acute hepatic failure*, Transpl Int, **15**, pp. 29-33.

[2] UNOS, (2005): *The US Organ Procurement and Transplantation Network and the Scientific Registry of Transplant Recipients*, OPTN / SRT Annual Report 2005.

[3] R. Williams, (1996): *Classification, etiology, and considerations of outcome in acute liver failure*, Semin Liver Dis, **16**, pp. 343-8.

[4] G. Catapano, (1996): *Mass transfer limitations to the performance of membrane bioartificial liver support devices*, Int J Artif Organs, **19**, pp. 18-35.

[5] L. M. Flendrig, F. Calise, E. Di Florio, A. Mancini, A. Ceriello, W. Santaniello, E. Mezza, F. Sicoli, G. Belleza, A. Bracco, S. Cozzolino, D. Scala, M. Mazzone, M. Fattore, E. Gonzales and R. A. Chamuleau, (1999): *Significantly improved survival time in pigs with complete liver ischemia treated with a novel bioartificial liver*, Int J Artif Organs, **22**, pp. 701-9.

ISSN: 1727-1983

[6] M. N. SOSEF, L. S. ABRAHAMSE, M. P. VAN DE KERKHOVE, R. HARTMAN, R. A. CHAMULEAU and T. M. VAN GULIK, (2002): *Assessment of the AMC-bioartificial liver in the anhepatic pig*, Transplantation, **73**, pp. 204-9.

[7] M. P. VAN DE KERKHOVE, E. DI FLORIO, V. SCUDERI, A. MANCINI, A. BELLI, A. BRACCO, M. DAURI, G. TISONE, G. DI NICUOLO, P. AMOROSO, A. SPADARI, G. LOMBARDI, R. HOEKSTRA, F. CALISE and R. A. CHAMULEAU, (2002): *Phase I clinical trial with the AMC-bioartificial liver*, Int J Artif Organs, **25**, pp. 950-9.

[8] U. J. BALIS, K. BEHNIA, B. DWARAKANATH, S. N. BHATIA, S. J. SULLIVAN, M. L. YARMUSH and M. TONER, (1999): *Oxygen consumption characteristics of porcine hepatocytes*, Metab Eng, **1**, pp. 49-62.